# New Two-Dimensional Manganese(II)-Azido Polymers with Bidentate Coligands: Structure and Magnetic Properties

En-Qing Gao,[†,‡] Yan-Feng Yue,[†,§] Shi-Qiang Bai,[†] Zheng He,[†] Shi-Wei Zhang,[†] and Chun-Hua Yan*[,†]

*State Key Laboratory of Rare Earth Materials Chemistry and Applications and PKU-HKU Joint Lab in Rare Earth Materials and Bioinorganic Chemistry, State Key Laboratory for Structural Chemistry of Unstable and Stable Species, Peking University, Beijing 100871, China, Shanghai Key Lab of Green Chemistry and Chemical Processes, East China Normal University, Shanghai 200062, China, and Department of Chemistry, Qufu Normal University, Qufu 273165, Shandong, China*

*Received November 12, 2003. Revised Manuscript Received February 6, 2004*

Two two-dimensional azido-bridged Mn(II) coordination polymers with bidentate coligands have been synthesized and structurally characterized, and their magnetic properties were studied. The complexes are of formula $[Mn(bphz)(N_3)_2]_n$ (**1**) and $[Mn(mipc)(N_3)_2]_n$ (**2**), where bphz = 2-benzoylpyridine hydrazone and mipc = methyl imidopyrazinecarboxylate. Both complexes consist of (6,3) layers in which double end-on (EO) azido-bridged dimers are interlinked by single end-to-end (EE) azido bridges, representing new examples of the sparse 2D Mn(II)-azido polymers assisted by bidentate coligands. Magnetic studies on the complexes reveal that ferromagnetic and antiferromagnetic interactions are mediated through the EO and EE azido bridges, respectively, with the global effect being antiferromagnetic. Both complexes exhibit spin canting related to the lack of inversion centers between the EE azido-bridged Mn(II) ions. Complex **1** behaves as a weak ferromagnet below 20 K, due to the long-range ordering of the residual spins originating from spin canting, but long-range ordering of the residual spins is not achieved in complex **2**.

## Introduction

The exceptional abilities of the azide anion as a versatile bridge to link two or more metallic centers in different modes (mainly EE and EO, Scheme 1) and as a good mediator to transmit antiferromagnetic (mainly for EE bridges) or ferromagnetic interactions (mainly for EO bridges), together with the remarkable diversities of the metal azido systems in polymeric dimensionality, topology, and bulk magnetic properties, have evoked considerable interest in the fields of molecular magnetism and coordination polymer chemistry.[1−3] Apart from discrete binuclear and polynuclear molecules,[4,5] one- (1D),[6−9] two- (2D),[10−12] and three-dimensional (3D)[13] polymeric complexes have been paid much attention in recent years. Different bridging modes and their appropriate combinations have provided a great

**Scheme 1. Different Bridging Modes of the Azido Ion**

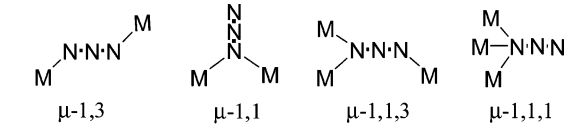


* To whom correspondence should be addressed. Fax: +86-10-62754179. E-mail: chyan@chem.pku.edu.cn.
† Peking University.
‡ East China Normal University.
§ Qufu Normal University.

(1) Miller, J. S., Drilon, M., Eds. *Magnetism: Molecules to Materials*; Willey-VCH: Weinheim, 2002.
(2) Kahn, O. *Molecular Magnetism*; VCH: New York, 1993.
(3) Ribas, J.; Escuer, A.; Monfort, M.; Vicente, R.; Cortés, R.; Lezama, L.; Rojo, T. *Coord. Chem. Rev.* **1999**, *193−195*, 1027 and references therein.
(4) (a) McLachlan, G. A.; Fallon, G. D.; Martin, R. L.; Moubaraki, B.; Murray, K. S.; Spiccia, L. *Inorg. Chem.* **1994**, *33*, 4663. (b) Rabis, J.; Monfort, M.; Kumar-Gosh, B.; Cortés, R.; Solans, X.; Font-Bardia, M. *Inorg. Chem.* **1996**, *35*, 864. (c) Lam, M. H. W.; Tang, Y. Y.; Fung, K. M.; You, X. Z.; Wong, W. T. *Chem. Commun.* **1997**, 957. (d) Serna, Z. E.; Lezama, L.; Urtiaga, M. K.; Arriortua, M. I.; Barandika, M. G. B.; Cortés, R.; Rojo, T. *Angew. Chem., Int. Ed.* **2000**, *39*, 344. (e) Escuer, A.; Goher, M. A. S.; Mautner, F. A.; Vicente, R. *Inorg. Chem.* **2000**, *39*, 2107.
(5) (a) Manikandan, P.; Muthukumaran, R.; Thomas, K. R. J.; Varghese, B.; Chandramouli, G. V. R.; Manoharan, P. T. *Inorg. Chem.* **2001**, *40*, 2378. (b) Papaefstathiou, G. S.; Escuer, A.; Raptopoulou, C. P.; Terzis, A.; Perlepes, S. P.; Vicente, R. *Eur. J. Inorg. Chem.* **2001**, 1567. (c) Halcrow, M. C.; Sun, J. S.; Huffman, J. C.; Christou, G. *Inorg. Chem.* **1995**, *34*, 4167. (d) Meyer, F.; Kircher, P.; Pritzkow, H. *Chem. Commun.* **2003**, 774.
(6) (a) Abu-Youssef, M. A.; Escuer, A.; Gatteschi, D.; Goher, M. A. S.; Mautner, F. A.; Vicente, R. *Inorg. Chem.* **1999**, *38*, 5716. (b) Escuer, A.; Vicente, R.; Goher, M. A. S.; Mautner, F. A. *Inorg. Chem.* **1998**, *37*, 782. (c) Mukherjee, P. S.; Dalai, S.; Zangrando, E.; Lloret, F.; Chaudhuri, N. R. *Chem. Commun.* **2001**, 1444.
(7) (a) Cortés, R.; Drillon, M.; Solans, X.; Lezama, L.; Rojo, T. *Inorg. Chem.* **1997**, *36*, 677. (b) Abu-Youssef, M.; Escuer, A.; Goher, M. A. S.; Mautner, F. A.; Vicente, R. *Eur. J. Inorg. Chem.* **1999**, 687. (c) Tang, L.-F.; Zhang, L.; Li, L.-C.; Cheng, P.; Wang, Z.-H.; Wang, J.-T. *Inorg. Chem.* **1999**, *38*, 6326. (d) Villanueva, M.; Mesa, J. L.; Urtiaga, M. K.; Cortés, R.; Lezama, L.; Arriortua, M. I.; Rojo, T. *Eur. J. Inorg. Chem.* **2001**, 1581.
(8) (a) Abu-Youssef, M.; Escuer, A.; Goher, M. A. S.; Mautner, F. A.; Reiss, G.; Vicente, R. *Angew. Chem., Int. Ed.* **2000**, *39*, 1624. (b) Abu-Youssef, M. A. M.; Drillon, M.; Escuer, A.; Goher, M. A. S.; Mautner, F. A.; Vicente, R. *Inorg. Chem.* **2000**, *39*, 5022. (c) Escuer, A.; Vicente, R.; El Fallah, M. S.; Goher, M. A. S.; Mautner, F. A. *Inorg. Chem.*, **1998**, *37*, 4466.

10.1021/cm0351590 CCC: $27.50 
Published on Web 03/19/2004

**Scheme 2. Different Types of 2D Azido-Bridged Networks**

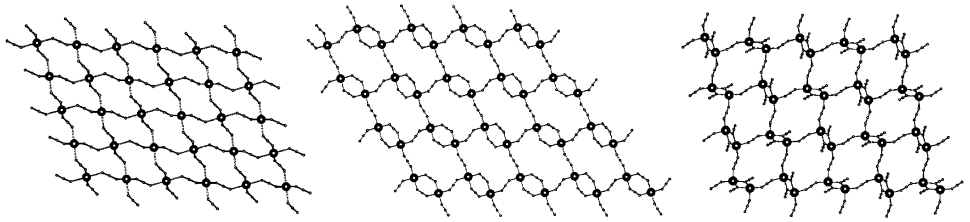

I II III

**Chart 1**

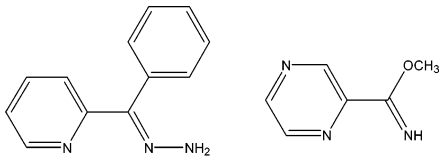


number of 1D azido-bridged systems with various topologies and magnetic properties, such as uniform AF or F chains,[6] alternating chains along which magnetic interactions alternate in different sequences (AF−F,[7] AF−AF−F,[8] AF−AF−F−F,[8c] or AF−F−F−F−F[8a]), and chains with more complicated topologies.[9] For 2D systems with only azido bridges, three kinds of topologies have been recognized to date (Scheme 2): (4,4) layers with only single EE azido bridges (type I),[10] (6,3) layers in which double EE azido-bridged dimers are interlinked by single EE bridges (type II),[11] and (6,3) layers in which double EO azido-bridged dimers are interlinked by single EE bridges (type III).[10a,11,12] Most of the 2D azido-bridged complexes are Mn(II) species, all of which are featured with dominant AF interactions via the EE bridge. It is interesting to note that some of the Mn(II) species exhibit weak ferromagnetic transitions with $T_c$ ranging from 16 to 30 K.[10c,d,11,12b]

The topology of a metal-azido system is obviously sensitive to the coligand. Despite the large number of M(II)-azido complexes reported to date, it seems impossible to predict a priori, with our present state of knowledge, the bridging mode or topology with a specific ligand. With monodentate ligands (usually pyridine and its derivatives), various Mn(II)-azido species with different dimensionalities or topologies have been obtained.[6−12,13a] With bidentate chelating coligands (Chart 1, however, we recently came to an impression that the resulting Mn(II)-azido complexes, of formula $[Mn(L)(N_3)_2]_n$, usually exhibit 1D chain structures with alternating double EO and double EE bridges.[6a,7c,d,14] The only exception reported previously is a 2D Mn(II)-azido layer compound of formula $[Mn(dmbpy)(N_3)_2]_n$ (dmbpy = 4,4′-dimethyl-2,2′-bipyridine).[10a] All other Mn(II)-azido 2D compounds are derived from monodentate ligands. In this report, we describe the structure and magnetic properties of two new 2D Mn(II)-azido layer complexes produced with bidentate ligands: 2-benzoylpyridine hydrazone (bphz) and methyl imidopyrazinecarboxylate (mipc). The chemical structures of the ligands are illustrated in Chart 1.

## Experimental Section

**Materials and Synthesis.** All the starting chemicals were of A. R. grade and used as received. The bphz ligand, 2-benzoylpyridine hydrazone, was prepared according to the literature methods.[15a] The mipc ligand, methyl imidopyrazinecarboxylate, was prepared under nitrogen atmosphere as follows:[15b,c] 2-cyanopyrazine (0.02 mol; 2.1 g) was added into a solution of sodium (0.060 g) in dry methanol (20 mL), and the mixture was stirred for 12 h at room temperature to yield white precipitate of the ligand, which was isolated by filtration and dried in a vacuum. The compound is stable in air. Anal. Calcd for $C_6N_3H_7O$: C, 52.55; H, 5.14; N, 30.64. Found: C, 52.36; H, 5.01; N, 30.95%. Main IR bands ($cm^{-1}$): 3284s, 1650vs, 1575m, 1449s, 1412s, 1378s, 1202m, 1020s. The observation of the strong band at 3284 $cm^{-1}$ indicates the presence of the NH group.

**CAUTION!** Although not encountered in our experiments, azido and perchlorate compounds of metal ions are potentially explosive. Only a small amount of the materials should be prepared, and it should be handled with care.

**$[Mn(bphz)(N_3)_2]_n$, 1.** The methanolic solution (10 mL) of manganese(II) perchlorate hexahydrate (0.25 mmol) was added into a solution of bphz (0.25 mmol) in the same solvent. The mixture was stirred for 15 min and then sodium azide (0.5 mmol) in 10 mL of methanol was added with continuous stirring. Slow evaporation of the resulting orange solution at room temperature yielded yellow crystals of **1** within 1 day. Yield, 35%. Anal. Calcd for $C_{12}H_{11}MnN_9$: C, 42.87; H, 3.30; N, 37.49. Found: C, 42.89; H, 3.21; N, 37.66%. Main IR bands ($cm^{-1}$): 3404m, 3295m, 2107s, 2062sh, 1593m, 1471m, 1334m, 789m, 706m.

**$[Mn(mipc)(N_3)_2]_n$, 2.** The complex was prepared in the same way as **1**, using the mipc ligand instead of bphz. Yield: 46%. Anal. Calcd for $C_6H_7N_9MnO$: C, 45.65; H, 2.56; N, 26.10. Found: C, 45.79; H, 2.75; N, 26.18%. Main IR band ($cm^{-1}$): 3279m, 2066vs, 1652m, 1383s, 1203m, 1137s, 1035m, 821m.

**Physical Measurements.** Elemental analyses (C, H, N) were performed on an Elementar Vario EL analyzer. IR spectra were recorded on a Nicolet Magna-IR 750 spectrometer equipped with a Nic-Plan Microscope. Temperature- and field-dependent magnetic measurements were carried out on an

(9) Zhang, L.; Tang, L.-F.; Wang, Z.-H.; Du, M.; Julve, M.; Lloret, F.; Wang, J.-T. *Inorg. Chem*. **2001**, *40*, 3619.

(10) (a) Escuer, A.; Vicente, R.; Goher, M. A. S.; Mautner, F. A. *J. Chem. Soc., Dalton Trans*. **1997**, 4431. (b) Goher, M. A. S.; Abu-Youssef, M. A.; Mautner, F. A.; Vicente, R.; Escuer, A. *Eur. J. Inorg. Chem*. **2000**, 1819. (c) Escuer, A.; Vicente, R.; Goher, M. A. S.; Mautner, F. A. *Inorg. Chem*. **1995**, *34*, 5707. (d) Escuer, A.; Vicente, R.; Goher, M. A. S.; Mautner, F. A. *Inorg. Chem*. **1996**, *35*, 6386.

(11) Escuer, A.; Cano, J.; Goher, M. A. S.; Journaux, Y.; Lloret, F.; Mautner, F. A.; Vicente, R. *Inorg. Chem*. **2000**, *39*, 4688.

(12) (a) Shen, Z.; Zuo, J. L.; Yu, Z.; Zhang, Y.; Bai, J. F.; Che, C. M.; Fun, H. K.; Vittal, J. J.; You, X. Z. *J. Chem. Soc., Dalton Trans*. **1999**, 3393. (b) Escuer, A.; Vicente, R.; Goher, M. A. S.; Mautner, F. A. *Inorg. Chem*. **1997**, *36*, 3440.

(13) (a) Goher, M. A. S.; Mautner, F. A. *Croat. Chem. Acta* **1990**, *63*, 559. (b) Goher, M. A. S.; Cano, J.; Journaux, Y.; Abu-Youssef, M. A.; Mautner, F. A.; Escuer, A.; Vicente, R. *Chem. Eur. J*. **2000**, *6*, 778. (c) Mautner, F. A.; Hanna, S.; Cortés, R.; Lezama, L.; Barandika, M. G.; Rojo, T. *Inorg. Chem*. **1999**, *38*, 4647.

(14) (a) Gao, E.-Q.; Bai, S.-Q.; Yue, Y.-F.; Wang, Z.-M.; Yan, C.-H. *Inorg. Chem*. **2003**, *42*, 3642. (b) Gao, E.-Q.; Bai, S.-Q.; Wang, C.-F.; Yue, Y.-F.; Yan, C.-H. *Inorg. Chem*. **2003**, *42*, 8456.

(15) (a) Bamfield, P.; Price, R.; Miller, R. G. J. *J. Chem. Soc. A* **1969**, 1447. (b) van Koningsbruggen, P. J.; Müller, E.; Haasnoot, J. G.; Reedijk, J. *Inorg. Chim. Acta* **1993**, *208*, 37. (c) Xu, Z.; Thompson, L. K.; Miller, D. O. *Inorg. Chem*. **1997**, *36*, 3985.

**Table 1. Summary of Crystallographic Data for the Complexes**

| | 1 | 2 |
|---|---|---|
| formula | $C_{12}H_{11}MnN_9$ | $C_6H_7MnN_9O$ |
| formula weight | 336.24 | 276.15 |
| crystal system | monoclinic | monoclinic |
| space group | $P2_1/c$ | $P2_1/c$ |
| $a$, Å | 10.8341(3) | 11.300(2) |
| $b$, Å | 10.2769(3) | 10.077(2) |
| $c$, Å | 13.0558(4) | 10.122(2) |
| $\beta$, deg | 103.0765(9) | 109.22(3) |
| $V$, Å$^3$ | 1415.95(7) | 1088.4(4) |
| $Z$ | 4 | 4 |
| $D_c$, g/cm$^3$ | 1.577 | 1.685 |
| $\mu$(Mo K$\alpha$), mm$^{-1}$ | 0.944 | 1.214 |
| $T$, K | 293(2) | 293 |
| $\theta$ range, deg | 3.41−27.47 | 2.78−27.47 |
| reflns measured | 27665 | 2393 |
| unique reflns/$R_{int}$ | 3226/0.0879 | 2393/0.00 |
| params refined | 207 | 154 |
| $R1^a$ [$I > 2\sigma(I)$] | 0.0378 | 0.0268 |
| $wR2^b$ (all data) | 0.0863 | 0.0521 |
| GOF on $F^2$ | 0.984 | 0.822 |
| $\rho_{max}/\rho_{min}$, e Å$^{-3}$ | 0.270/−0.343 | 0.262/−0.318 |

$^a$ $R1 = \sum||F_o| - |F_c||/\sum|F_o|$. $^b$ $wR2 = \{\sum[w(F_o^2 - F_c^2)^2]/\sum[w(F_o^2)^2]\}^{1/2}$.

Oxford MagLab 2000 magnetometer. Diamagnetic corrections were made with Pascal's constants.[16]

**Crystallographic Studies.** Diffraction intensity data for single crystals were collected at room temperature on a Nonius Kappa CCD area detector (**1**) and a Rigaku RAXIS RAPID IP diffractometer (**2**), both equipped with graphite-monochromated Mo K$\alpha$ radiation ($\lambda = 0.71073$ Å). Empirical absorption corrections were applied.[17] The structure was solved by the direct method and refined by the full-matrix least-squares method on $F^2$ with anisotropic thermal parameters for all non-hydrogen atoms.[18] Hydrogen atoms were located geometrically and refined using the riding model. Pertinent crystallographic data and refinement parameters are summarized in Table 1.

## Results and Discussion

**Synthesis and IR Spectra.** The complexes were prepared as crystals by slow evaporation of the mixture solutions containing manganese(II) perchlorate, the corresponding ligands, and sodium azide. The synthetic procedures are similar to those we used previously for preparing Mn(II)-azido complexes with the Schiff bases derived from the condensation of 2-pyridylaldehyde with aniline, *p*-toluidine, *m*-toluidine, *p*-chloroaniline, and *m*-chloroaniline.[14] All of the present and previous complexes contain bidentate coligands and exhibit the same general formula of $[Mn(L)(N_3)_2]_n$. However, the previous complexes are all 1D chain compounds with alternating double EO and double EE azido bridges, whereas the present complexes are 2D layer compounds with alternating double EO and single EE bridges. The reason the use of bphz and mipc leads to 2D complexes, instead of 1D ones, is unclear, and any correlation between the ligand properties and the structure of the complexes may be unwarranted with so few examples.

The IR spectra of the complexes display characteristic bands of the azido bridges and the C═N group. In the region expected for the $\nu_{as}(N_3)$ absorption, complex **1** exhibits two sharp and strong bands at 2062 and 2107 cm$^{-1}$, attributable to the EE bridge and the EO bridge, respectively.[7,19] Complex **2** exhibits a very strong band at 2066 cm$^{-1}$, with a small shoulder at the higher frequency side, also indicating the presence of the two different azido groups. The absorptions of the C═N stretching vibration in the ligands occur as medium bands at 1593 and 1652 cm$^{-1}$ for **1** and **2**, respectively. The two medium absorptions at 3404 and 3295 cm$^{-1}$ of **1** are assignable to the $\nu_{as}(NH_2)$ and $\nu_s(NH_2)$ modes of the bphz ligand, whereas the $\nu$(NH) absorption of the mipc ligand in **2** is observed as a medium band at 3279 cm$^{-1}$.

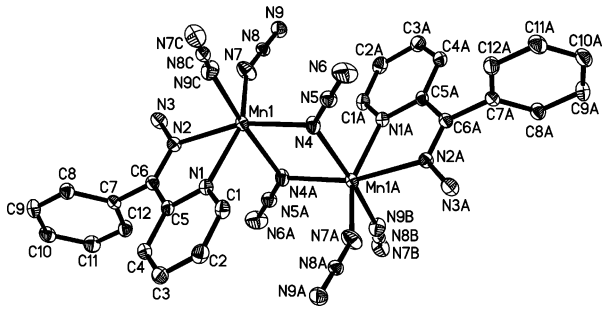


**Figure 1.** Binuclear building unit in complex **1** with atom labeling scheme. The thermal ellipsoids were drawn at 30% probability.

**Description of the Structures.** Single-crystal X-ray analyses revealed that complex **1** consists of (6,3) layers of type III (Scheme 2). A perspective view of the binuclear unit is shown in Figure 1, and selected bond lengths and angles are listed in Table 1.

Each Mn(II) ion is ligated by a pyridyl nitrogen, an imine nitrogen, and four azido nitrogens, with the Mn−N distances ranging from 2.168(2) to 2.291(2) Å. The aromatic phenyl and pyridyl rings of each bphz ligand are nearly perpendicular to each other with a dihedral angle of 96.7°, and the hydrazone group is coplanar with the pyridyl ring. The pseudo-octahedral coordination geometry is *cisoid* and highly distorted: the bite angle of the bidentate Schiff base (N1−Mn1−N2, 70.9°), the *cisoid* N7(azido)−Mn1−N4(azido) angle (108.1°), and the *transoid* N7(azido)−Mn1−N1(pyridyl) angle (155.1°) deviate significantly from the ideal values (90° or 180°). Two neighboring Mn(II) ions related by an inversion center are doubly linked by two azido ions in the end-on mode, forming a binuclear building unit (Figure 1). In the resulting $Mn_2N_2$ planar parallelogrammic ring, the Mn−N−Mn bridging angle is 101.9°, and the Mn···Mn distance is 3.459 Å. These values lie in the typical range for double EO azido bridges.[14] Each binuclear unit is connected to four neighboring identical units through four azido bridges in the end-to-end mode, generating a 2D layer parallel to the *bc* plane, with a honeycomb (6,3) topology (Figure 2, each Mn atom as a node). The neighboring $Mn_2$ units are interrelated by a $2_1$ screw operation, and the acute dihedral angle between their $Mn_2N_2$ planar rings is 78.9°. An alternative description of the structure is that the layer consists of EE azido-bridged Mn($N_3$) helical chains interlinked by double EO azido bridges. The helical chain runs around a 2-fold screw axis in the *b* direction, and neighboring

(16) O'Connor, C. J. *Prog. Inorg. Chem.* **1982**, *29*, 203.
(17) (a) Blessing, R. H. *Acta Crystallogr.* **1995**, *A51*, 33. (b) Blessing, R. H. *J. Appl. Crystallogr.* **1997**, *30*, 421.
(18) (a) Sheldrick, G. M. SHELXTL Version 5.1. Bruker Analytical X-ray Instruments Inc.: Madison, WI, 1998. (b) Sheldrick, G. M. SHELXL-97, PC Version; University of Göttingen, Germany, 1997.
(19) Tandon, S. S.; Thompson, L. K.; Manuel, M. E.; Bridson, J. N. *Inorg. Chem.* **1994**, *33*, 5555.

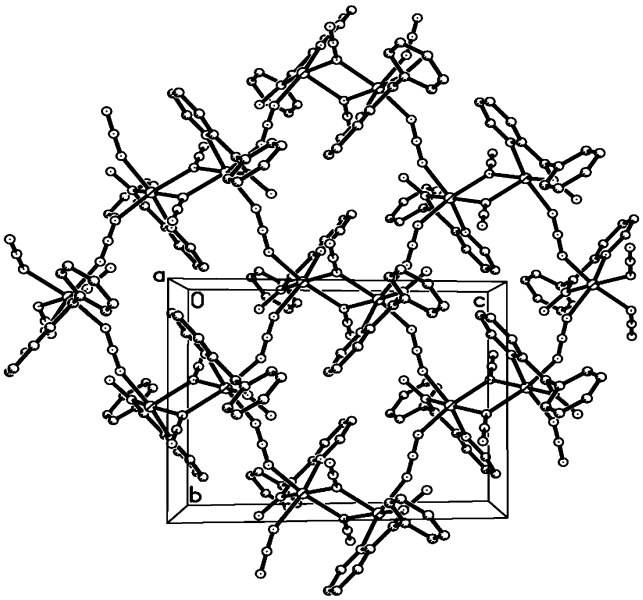


**Figure 2.** 2D layer in complex **1**.

chains are related by inversion centers and have opposite chirality. Within the chain, the Mn−N−N angles are 158.1(2) and 150.94(2)°, the N−Mn−N angle is 92.22(9)°, and the Mn−N−N−N−Mn torsion angle is 158.5°. The Mn···Mn distance spanned by the EE bridge is 6.496 Å, and the helical pitch is equal to the *b* dimension [10.2769(3) Å]. Both EO and EE azido bridges are essentially linear, but the EO bridge exhibits typical asymmetric N−N distances [1.196(2) and 1.150(3) Å] and the EE bridge exhibits identical N−N distances [1.158(3) Å], consistent with the coordination modes.

In the crystal, the 2D layers are stacked down the *a* direction, with the minimum interlayer Mn···Mn distance being 10.349 Å—significantly shorter than the distances found in most 2D Mn-azido systems (typically between 13 and 17 Å). This short interlayer separation in **1** may be a consequence of deep complementary interdigitation between consecutive layers. As can be seen from Figure 3 (top), the phenyl groups of the bphz ligands on each side of a layer extend deeply into the "empty" space of neighboring layers. A closer inspection reveals that the interdigitation is sustained by $\pi-\pi$ interactions: each phenyl ring from a layer overlaps partly with the adjacent pyridyl ring from a neighboring layer, and each binuclear unit of a layer interacts with four units from the two neighboring layers (Figure 3, bottom). The dihedral angle between the interacting aromatic rings is 15.9° and the centroid−centroid distance is 3.92 Å. As shown in Figure 3 (bottom), the weak $\pi-\pi$ interactions generate helical supramolecular chains of bphz ligands along $2_1$ screw axes parallel to the *b* direction.

Compound **2** also consists of 2D Mn-azido layers of type III. The binuclear unit and the layer structure are shown in Figure 4. The geometrical parameters of the metal sphere are similar to those in **1**, with the largest difference being the N4−Mn1−N7 angles, and the double EO bridging moieties in **1** and **2** show no appreciable differences in the Mn−N−Mn angle and the Mn···Mn distance. However, they differ significantly from each other in the EE bridging moiety. In **2**, the Mn−N−N angles are much smaller (Table 2), and the

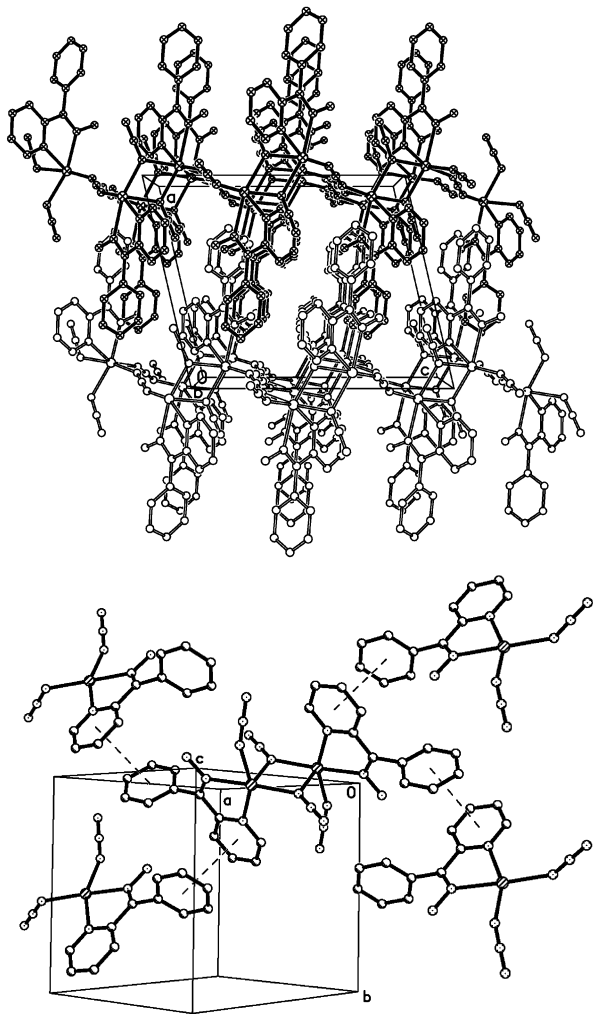


**Figure 3.** Interdigitation between neighboring layers (top) and the $\pi-\pi$ interactions between a binuclear unit and its neighbors (bottom) in **1**.

Mn−$N_3$−Mn torsion angle is much less obtuse (92.4 vs 158.5°), and hence the Mn···Mn distance is significantly shorter (5.648 vs 6.496 Å). The 2D layers in **2** are also parallel to the *bc* crystallographic plane, with the minimum interlayer Mn···Mn distance being 10.392 Å. This value is comparable to that in **1**, but there are no evident interlayer $\pi-\pi$ interactions or hydrogen bonds.

**Magnetic Properties.** *Complex **1***. The magnetic susceptibility of compound **1** was measured in the 2−300 K range at 5000 G and shown as $\chi_M$-*T* and $\chi_M T$-*T* plots in Figure 5. The high-temperature susceptibility above 60 K obeys the Curie−Weiss law with $\theta = -54.2$ K and $C = 4.7$ emu mol$^{-1}$ K (See Figure S1 in Supporting Information). The negative Weiss constant indicates that the overall interaction is antiferromagnetic. The $\chi_M T$ value at 300 K is ca. 3.98 emu K mol$^{-1}$, lower than the spin-only value (4.38 emu K mol$^{-1}$) expected for a magnetically isolated high-spin Mn(II) ion with $g = 2.00$. Upon cooling, $\chi_M T$ decreases monotonically and vanishes when *T* approaches zero, indicating an overall antiferromagnetic interaction. But the temperature dependence of the susceptibility is more complex. As the temperature is lowered, $\chi_M$ first increases to a rounded maximum of 0.047 emu mol$^{-1}$ at about 33 K, then decreases to a minimum value of 0.044 emu mol$^{-1}$ at 20 K, and finally increases rapidly to 0.059

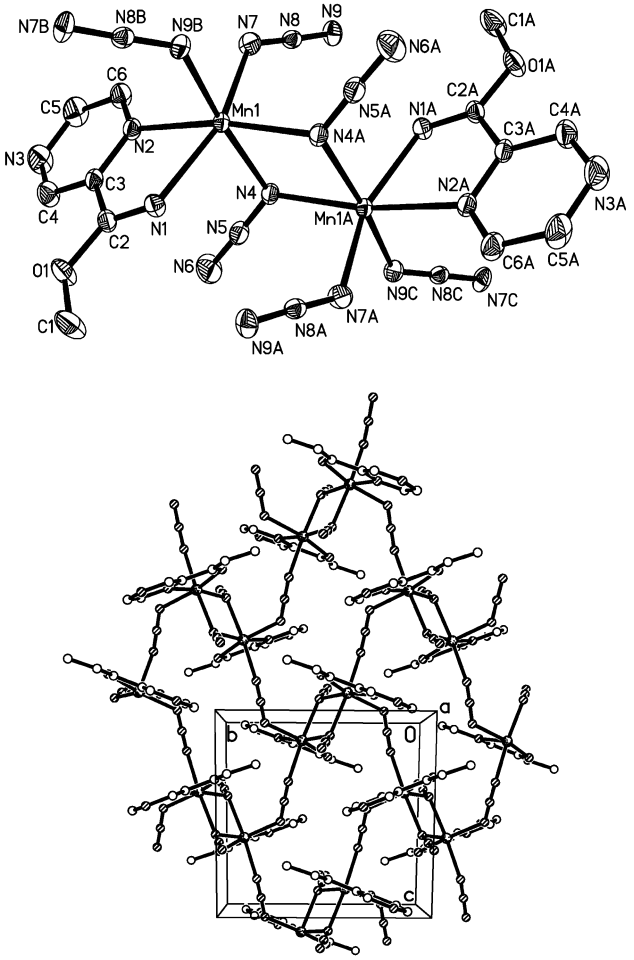


**Figure 4.** Binuclear building unit (top) and the 2D layer (bottom) in **2**.

emu mol$^{-1}$ at 2 K. The behaviors above 20 K are typical of 1D and 2D Mn(II) complexes with dominant antiferromagnetic interactions, and the abrupt increase of $\chi_M$ below 20 K may be due to the presence of a spin-canted structure (vide infra).

No analytical expression of magnetic susceptibility is available for this kind of 2D Mn(II) layer. To evaluate the magnetic interactions, we applied an approximate approach based on the structural and magnetic data. It has been established that the azido bridge usually mediates an antiferromagnetic interaction when the EE bridging mode is adopted, but the interaction is usually ferromagnetic when the EO mode is adopted. Although there have been a few exceptions in some Cu(II) and Ni(II) species, where the nature of the interaction is sensitive to the structural parameters of the bridge and/or the metal environment, no exception has been found in Mn(II) species. Therefore, it seems safe to assume that the present compound exhibits ferro- and antiferromagnetic interactions through double EO and single EE azido bridges, respectively. Because the temperature dependence of the susceptibility has revealed that antiferromagnetic interaction dominates, it is reasonable to consider the EE bridge first. As has been mentioned, the EE bridges interlink the Mn(II) ions into a uniform chain, so we treated the 2D layer as EE azido-bridged antiferromagnetic chains interacting ferromagnetically through the double EO azido bridges. For the intrachain antiferromagnetic interaction ($J$), we used

**Table 2. Selected Bond Lengths and Angles for Complexes 1 and 2**[a]

| | 1 | 2 |
|---|---|---|
| Mn(1)−N(1) | 2.2738(18) | 2.2294(15) |
| Mn(1)−N(2) | 2.2907(17) | 2.3378(15) |
| Mn(1)−N(4) | 2.1883(19) | 2.1878(15) |
| Mn(1)−N(4A) | 2.265(2) | 2.2588(18) |
| Mn(1)−N(7) | 2.168(2) | 2.1928(19) |
| Mn(1)−N(9B) | 2.175(2) | 2.1998(17) |
| N(4)−N(5) | 1.196(2) | 1.198(2) |
| N(5)−N(6) | 1.150(3) | 1.150(2) |
| N(7)−N(8) | 1.158(3) | 1.173(2) |
| N(8)−N(9) | 1.158(3) | 1.170(2) |
| N(1)−Mn(1)−N(2) | 70.93(6) | 71.93(6) |
| N(1)−Mn(1)−N(4) | 96.61(7) | 104.96(6) |
| N(1)−Mn(1)−N(4A) | 87.70(7) | 88.91(6) |
| N(1)−Mn(1)−N(7) | 155.13(7) | 156.99(6) |
| N(1)−Mn(1)−N(9B) | 89.69(8) | 92.55(6) |
| N(2)−Mn(1)−N(4) | 163.53(8) | 167.95(6) |
| N(2)−Mn(1)−N(4A) | 90.36(7) | 89.02(6) |
| N(2)−Mn(1)−N(7) | 84.26(7) | 85.09(6) |
| N(2)−Mn(1)−N(9B) | 98.08(7) | 98.02(7) |
| N(4)−Mn(1)−N(4A) | 78.11(7) | 79.22(7) |
| N(4)−Mn(1)−N(7) | 108.07(8) | 97.77(6) |
| N(4)−Mn(1)−N(9B) | 92.44(8) | 93.72(7) |
| N(4A)−Mn(1)−N(7) | 94.29(9) | 91.90(7) |
| N(4A)−Mn(1)−N(9B) | 169.82(8) | 172.93(6) |
| N(7)−Mn(1)−N(9B) | 92.22(9) | 89.46(7) |
| N(5)−N(4)−Mn(1) | 128.23(17) | 126.62(14) |
| N(5)−N(4)−Mn(1A) | 129.72(16) | 118.82(13) |
| Mn(1)−N(4)−Mn(1A) | 101.89(7) | 100.78(7) |
| N(8)−N(7)−Mn(1) | 158.1(2) | 131.67(14) |
| N(8)−N(9)−Mn(1C) | 150.94(19) | 132.27(14) |

[a] Symmetry Codes for **1**: (A) $-x+2, -y, -z+1$; (B) $-x+2, y-1/2, -z+3/2$; (C) $-x+2, y+1/2, -z+3/2$. For **2**: (A) $-x+1, -y, -z+1$; (B) $x, -y+1/2, z-1/2$; (C) $x, -y+1/2, z+1/2$.

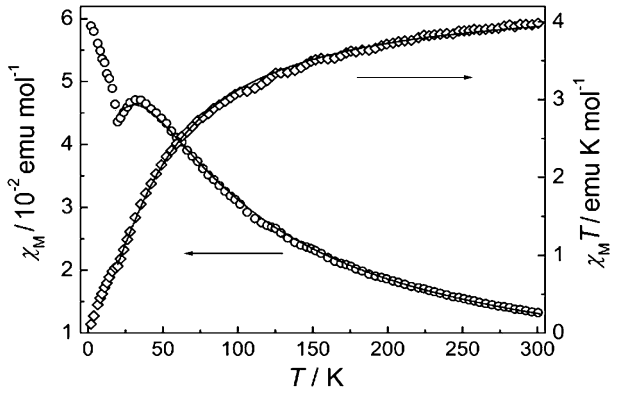


**Figure 5.** Temperature dependence of $\chi_M$ and $\chi_M T$ for **1**. The solid lines represent the best fit of the experimental data to eqs 1 and 2.

the theoretical expression proposed by Fisher for 1D uniform chains:[20]

$$\chi_{chain} = [Ng^2\beta^2 S(S+1)/(3kT)][(1+u)/(1-u)] \quad (1)$$

where $u = \coth[JS(S+1)/kT] - kT/[JS(S+1)]$ and $S = 5/2$. The $J$ parameter is based on the spin Hamiltonian $\boldsymbol{H} = -J\Sigma \boldsymbol{S}_i \boldsymbol{S}_{i+1}$, and the $\boldsymbol{S}$ operator is treated as a classical spin. The interchain interaction ($zJ'$) through the EO bridges was treated by the molecular field approximation[16]

$$\chi = \chi_{chain}/[1 - (zJ'/Ng^2\beta^2)\chi_{chain}] \quad (2)$$

(20) Fisher, M. E. *Am. J. Phys.* **1964**, *32*, 343.

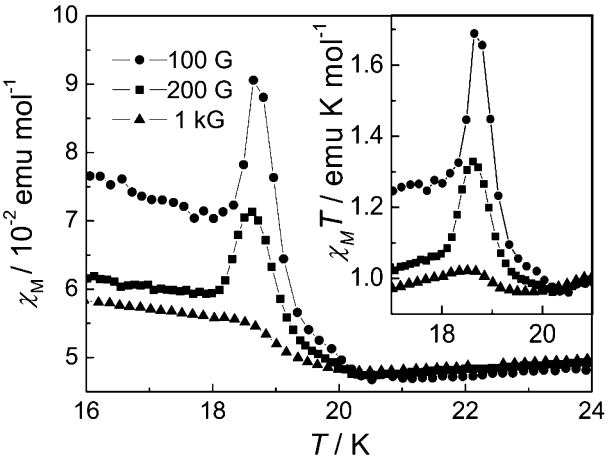


**Figure 6.** Field-cooled $\chi_M$ and $\chi_M T$ (inset) versus $T$ plots at different fields for **1**.

The least-squares fit of the experimental data above 20 K to the above expressions led to $J = -5.1(1)$ $cm^{-1}$, $zJ' = 3.1(2)$ $cm^{-1}$ with $g = 2.00(1)$. These values confirm that the interactions mediated via the single EE and the double EO bridges are antiferro- and ferromagnetic, respectively. However, it should be noted that the fitted values for $J$ and $zJ'$ are only qualitatively valid, because their comparability in magnitude does not meet the requirement of the molecular field approximation that $zJ'$ should be much smaller than $J$.[16]

The magnetic behavior in the low-temperature region deserves further investigation. Field-cooled magnetization measurements were performed under different fields (Figure 6). Under lower fields of 100 and 200 G, both the magnetic susceptibility ($\chi_M = M/H$) and its product with temperature ($\chi_M T$) exhibit abrupt increases below 20 K, and reach maximums at about 18.5 K. The maximums are lowered when the applied field is increased. At a higher field of 1 kG, the maximum of $\chi_M$ disappears, whereas that of $\chi_M T$ remains. The abrupt increase in $\chi_M T$ below 20 K indicates that there exists a ferromagnetic-like correlation. The weak ferromagnetism may be attributed to spin canting,[3] i.e., perfect antiparallel alignment of the spins on the antiferromagnetically coupled metal ions is not achieved so that a spin-canted structure is generated within the layer, resulting in residual spins. The increase in $\chi_M T$ below 20 K indicates a ferromagnetic-like correlation is operative between the residual spins. The presence of the maximum in $\chi_M$ at lower fields may be due to antiferromagnetic interactions between the spin-canted layers, and the disappearance of the maximum at higher fields may suggest that the antiferromagnetic interactions are overcome by the external field, indicative of a metamagnetic-like behavior. At the field of as high as 5 kG, the $\chi_M$ value still shows an abrupt increase below 20 K (Figure 5), suggesting the spin-canting remains in operation, but $\chi_M T$ decreases monotonically and shows no maximum anymore (a change in the curvature is still evident), suggesting that the ferromagnetic-like correlation between the residual spins is almost overcome by the external field. Field-dependent magnetization was also measured at 2.0 K (Figure 7). The magnetization curve exhibits evident nonlinearity, with an inflection point at around 20 kG, which should be related to the spin flop behavior. The magnetization reached at 50 kG

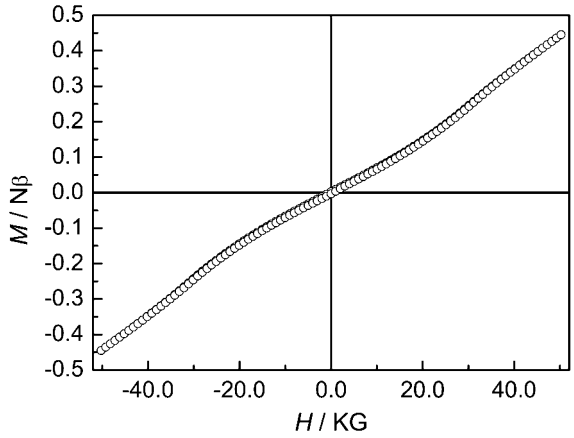


**Figure 7.** Field dependence of magnetization of **1** measured by cycling the field between +50 and −50 kG at 2 K.

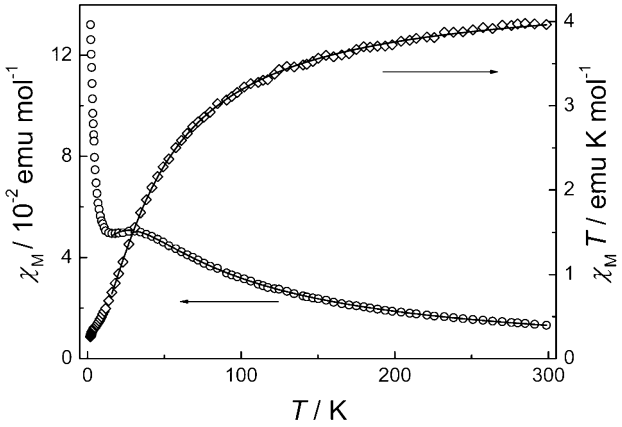


**Figure 8.** Temperature dependence of $\chi_M$ and $\chi_M T$ for **2**. The solid lines represent the best fit of the experimental data to eqs 1 and 2.

is only 0.45 N$\beta$, far below the saturation value expected for an $S = {}^5/_2$ system (5 N$\beta$ with $g = 2.0$). No hysteresis was detected.

**Complex 2.** The temperature-dependent magnetic behaviors of compound **2** in the 2−300 K range are shown in Figure 8. The high-temperature susceptibility above 60 K obeys the Curie−Weiss law with $\theta = -44.9$ K and $C = 4.6$ emu $mol^{-1}$ K (See Figure S1 in Supporting Information), suggesting an overall antiferromagnetic interaction. Although the general features resemble those of **1**, there are some significant differences. The maximum and minimum of the $\chi_M$-$T$ plot for **2** are more rounded and occur at lower temperature values (around 28 and 16 K, respectively), and the $\chi_M$ value (0.13 emu $mol^{-1}$) reached at 2 K is much higher than that for **1**. The least-squares fits of the experimental data of **2** above 16 K to eqs 1 and 2 led to $J = -4.6(1)$ $cm^{-1}$, $zJ' = 2.2(1)$ $cm^{-1}$ with $g = 2.00(1)$, confirming the antiferro- and ferromagnetic interactions through the single EE and the double EO azido bridges. Again, these values for $J$ and $zJ'$ should be only qualitatively valid.

Field-cooled magnetization measurements in the low-temperature region were also performed on **2** at lower fields (see Figure S2 in Supporting Information). Upon decreasing the temperature below 16 K, the $\chi_M$ value increases smoothly, and the $\chi_M T$ product decreases continuously and shows no increase. Moreover, the field-

**Table 3. Structural and Magnetic Parameters for 2D Mn(II) Complexes of Type III**

| complex[a] | **1** | **2** | **3** | **4** | **5** | **6** | **7** |
|---|---|---|---|---|---|---|---|
| space group | $P2_1/c$ | $P2_1/c$ | $P2_1/a$ | $P2_1/c$ | $P2_1/a$ | $P2_1/c$ | $P2_1/n$ |
| canting | yes | yes | yes | yes | yes | yes | no |
| $T_C$, K | 19.5 | no | 18 | 16 | 16 | 20 | no |
| hysteresis | no | no | no | yes | yes | yes | no |
| $J_{EE}$, $cm^{-1}$ | −5.1 | −4.6 | | | | −5.3 | −5.4 |
| $J_{EO}$, $cm^{-1}$ | 3.1 | 1.1 | | | | 2.9 | 1.7 |
| α, deg[b] | 78.9 | 83.7 | 20.9 | 81.9 | 67.5 | 86.7 | 0 |
| τ, deg[c] | 158.5° | 92.4 | 58.0 | 65.3 | 55.3 | 17.6 | 180 |
| M−N−M, deg[d] | 101.9 | 100.8 | 100.5° | 104.1° | 103.4, | 102.2 | 102.2 |
| M−N−N, deg[e] | 158.1 | 131.7 | 129.4 | 149.4° | 157.2 | 150.3° | 163.8 |
| | 150.9 | 132.3 | 141.1 | 140.1 | 139.7 | 143.9 | 153.9 |
| M···M(EO), Å | 3.459 | 3.426 | 3.425 | 3.556 | | 3.523 | 3.533 |
| M···M(EE), Å | 6.496 | 5.648 | 5.712 | 6.195 | | 6.083 | 6.611, 6.537 |
| *D*, Å[f] | 10.349 | 10.392 | 13.579 | 11.268 | 15.760 | 13.274 | 9.893 |
| ref. | this work | this work | 12b | 12b | 10d | 11 | 12a |

[a] $[Mn(NN)(N_3)_2]_n$: NN = 2-benzoylpyridine hydrazone (**1**), methyl imidopyrazinecarboxylate (**2**), and 4,4′-dimethyl-2,2′-bipyridine (**7**). $[Mn(L)_2(N_3)_2]_n$: L = 4-cyanopyridine (**3**), 3-acetylpyridine (**4**), ethyl-isonicotinate (**5**), and 4-ethylpyridine (**6**). [b] The dihedral angle between the neighboring planar $Mn_2N_2$ rings. [c] The M−N−N−M torsion angle. [d] For the EO azido bridging moiety. [e] For the EE azido bridging moiety. [f] Interlayer Mn···Mn distances.

cooled magnetization curve is independent of the applied field. Field dependent magnetization was also measured at 2 K. The magnetization reached at 50 kG is 0.52 N$\beta$, and no hysteresis was observed (see Figure S2 in Supporting Information). These magnetic behaviors, quite different from those of **1**, are indicative of a spin-canted antiferromagnetic system without long-range ordering: the spin-canting effect between antiferromagnetically coupled Mn(II) ions leads to residual spins, which are responsible for the increase in $\chi_M$ at low temperature, but no long-range ordering between the residual spins is achieved. The occurrence of spin canting is supported by the structural consideration presented in the following paragraph.

**Spin Canting Consideration.** To our knowledge, only five Mn(II)-azido 2D networks with double EO and single EE bridges (type III, as we have classified) have been synthesized and characterized previously. Four of the complexes, of formula $[Mn(L)_2(N_3)_2]_n$ (Table 3, **3**−**6**), which are different from **1** and **2** in that they contain monodentate coligands and *trans*-octahedral metal centers, were reported to exhibit weak ferromagnetism due to spin canting, with $T_c$ between 16 and 20 K. However, the last complex, $[Mn(dmbpy)(N_3)_2]_n$ (**7**), which is similar to **1** and **2** in that it also contains a bidentate coligand and *cis*-octahedral Mn(II) centers, does not exhibit spin-canting behavior. It is worthwhile to gain an insight into the structural origin of the magnetic differences. It is well-known that spin canting may arise from two mechanisms: (i) single-ion magnetic anisotropy, and (ii) antisymmetric exchange.[21] Because of the isotropic character of the high spin Mn(II) ion, the second factor should be responsible for the canting in compounds **1**−**6**. It has been formulated that the antisymmetric exchange vanishes when an inversion center is present between neighboring spin centers.[21] We noted that all of the seven complexes crystallize in the same centrosymmetric space group (No. 14, reported as $P2_1/c$, $P2_1/n$, or $P2_1/a$), and exhibit similar 2D networks of type III. However, a closer inspection reveals that compound **7** differs significantly from the others in local symmetry. In compounds **1**−**6**, although the Mn(II) ions linked by the EO azido bridges are related by inversion centers, there are no inversion centers between the metal centers linked by the single EE azido bridge. It is expected that an antisymmetric exchange between the EE-azido bridged Mn(II) ions is operative and superimposed upon the isotropic antiferromagnetic exchange, leading to the observed spin-canting phenomenon. In **7**, however, each EE azido bridge lies on an inversion center, so that all neighboring Mn(II) ions, whether they are linked by EE or EO azido bridge, are interrelated by inversion centers. Therefore, the antisymmetric exchange vanishes, and no spin-canting behavior is observed. An alternative justification is to describe the structure as double EO-azido bridged $Mn_2$ units being interlinked by EE azido bridges. Because the interaction between Mn(II) ions through double EO azido bridges is ferromagnetic, each $Mn_2$ unit may be viewed as a high-spin center. In complexes **1**−**6**, neighboring $Mn_2$ units are interrelated by screw axes and have different orientations. The dihedral angle between neighboring planar $Mn_2N_2$ rings ranges from 20.9° to 86.7° (Table 3). Thus, the antisymmetric exchange between neighboring $Mn_2$ units is possible and leads to spin canting. In **7**, however, neighboring $Mn_2$ units are interrelated by inversion centers, and hence spin canting does not occur.

We also listed some other structural and magnetic data of complexes **1**−**7** in Table 3, attempting to find certain magneto−structural correlations such as those concerning $T_c$, $J$, etc. However, with the rather limited data, it seems that no conclusive remarks are warranted.

**Acknowledgment.** We thank NSFC (20201009, 20221101, and 20391001) for the financial support.

**Supporting Information Available:** Crystallographic data (CIF) and magnetic plots for compounds **1** and **2** (pdf). This material is available free of charge via the Internet at http://pubs.acs.org.

CM0351590

(21) (a) Dzyaloshinsky, I. *Phys. Chem. Solids* **1958**, *4*, 241. (b) Moriya, T. *Phys. Rev.* **1960**, *120*, 91. (c) Armentano, D.; Munno, G. D.; Lloret, F.; Palli, A. V.; Julve, M. *Inorg. Chem.* **2002**, *41*, 2007.